Dalton Transactions



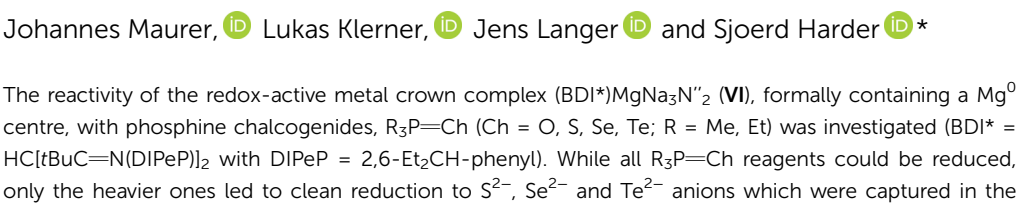
View Article Online **PAPER**



Cite this: Dalton Trans., 2025, 54. 13950

Received 8th August 2025, Accepted 2nd September 2025 DOI: 10.1039/d5dt01896j

chalcogenides



centre, with phosphine chalcogenides, $R_3P = Ch$ (Ch = O, S, Se, Te; R = Me, Et) was investigated (BDI* = HC[tBuC=N(DIPeP)]2 with DIPeP = 2,6-Et2CH-phenyl). While all R3P=Ch reagents could be reduced, only the heavier ones led to clean reduction to S^{2-} , Se^{2-} and Te^{2-} anions which were captured in the metalla-cycle. The smaller S^{2-} anion can be stabilized by the tetrametallic MqNa₃-crown but the larger Se^{2-} and Te^{2-} require a pentametallic MgNa₄-crown. Reaction of the sulfide complex with N₂O led to a rare thiohyponitrite cis-SNNO²⁻ anion which is trapped in the pentametallic MgNa₄-crown. Experimental observations and bonding characteristics of all complexes are supported by an additional computational study.

Redox-active inverse crowns – pockets for heavier

Introduction

rsc.li/dalton

Classic crown ethers like 18-crown-6 developed by Pedersen effectively bind metal cations within their polyether cavity (I, Scheme 1a - top). 1-3 In contrast, inverse crown ethers inverse this concept and trap anions within a cavity spanned by metal cations (II, Scheme 1a - bottom). Seminal reports by Mulvey and coworkers describe the serendipitous self-assembly of inverse crown ethers by reaction of NaⁿBu, Mg(ⁿBu)₂ and HN" $(N'' = [N(SiMe_3)_2]^{-})$ and small quantities of oxygen impurities like O₂ or H₂O.^{4,5} Such complexes are generally formed in low yields and often mixtures of oxides and peroxides are obtained. These initial investigations have been extended to capturing more complex moieties within the metal crown, enabling the synthesis of unique multi-anionic products that are not accessible by standard deprotonation methods.6

Although the first inverse crown ethers with O²⁻ core anions have been extensively investigated, similar metal crown complexes with heavier chalcogenide anions (S²⁻, Se²⁻, Te²⁻) have so far not been reported. There is in general a lack of information on polar s-block metal complexes with heavy chalcogenides. The Cambridge Crystallographic Database contains only three crystal structures of s-block metal complexes with sulfide anions, i.e. complex III-S (Scheme 1b) and solvates thereof.^{7,8} For polar selenide complexes there are only two examples, III-Se and the scorpionate complex IV (Scheme 1b).8,9 s-Block metal complexes with encapsulated

Te²⁻ anions are completely unknown. There are rare reports for the more polar molecular aluminium complexes with heavier chalcogenide anions (e.g. V-Ch, Scheme 1b). 10-12 This lack of knowledge stands in strong contrast with transition metal chalcogenide chemistry for which complexes13-22 and materials²³ have been well studied.

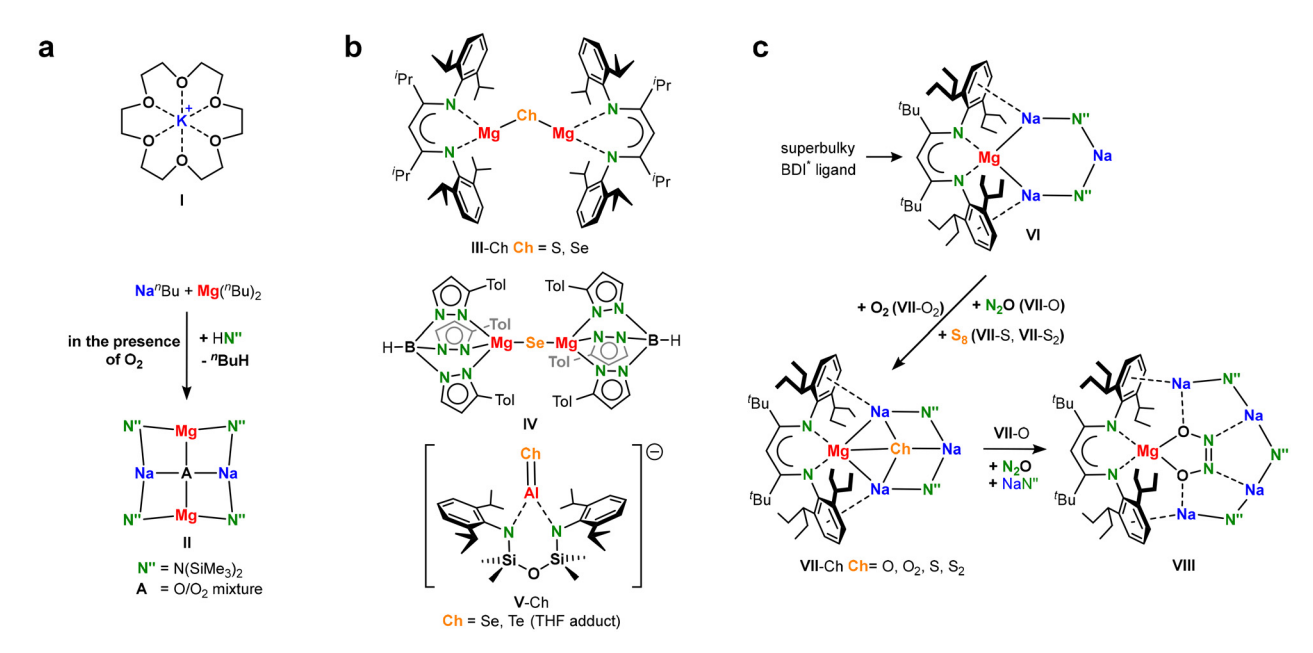
Herein, we present a unique "reduce-and-capture" concept to access ionic s-block metal complexes of the heavier chalcogenides Ch2- anions. We recently introduced a redox-active metal crown complex (VI, Scheme 1c) that is able to reduce a substrate and encapsulate the resulting dianion.²⁴ This was exemplary shown for reaction with N₂O or epoxides, producing the O²⁻ anion, or for reaction with O₂ to give an encapsulated peroxide dianion. Depending on stoichiometry, reactions with S_8 resulted either in reduction to S^{2-} or formation of S_2^{2-} . Herein, we extend these investigations aiming to isolate complexes with a Se²⁻ anion, which are rare, or a Te²⁻ anion, which are hitherto unknown. As the ionic radii of the Ch²⁻ dianions gradually increase from O²⁻ (1.40 Å) over S²⁻ (1.84 Å) and Se^{2-} (1.98 Å) to Te^{2-} (2.21 Å) by almost 58%, 25 we were particularly interested whether capturing these larger anions requires ring extension. We also discuss trends in crystal structures, discuss solution dynamics and support our findings with DFT calculations.

Results and discussion

Phosphine chalcogenides, R₃P=Ch, have been shown to be potent chalcogen transferring agents.8,10-12,26-32 The key to this reactivity lies within the P=Ch bond which strictly speaking has more ylid (P⁺-Ch⁻) than ylene character and weakens

Inorganic and Organometallic Chemistry, Friedrich-Alexander-Universität Erlangen-Nürnberg, Egerlandstraße 1, 91058 Erlangen, Germany. E-mail: sjoerd.harder@fau.de

Dalton Transactions Paper



Scheme 1 (a) From Pedersen's crown ethers¹⁻³ to Mulvey's inverse crown complexes.⁴⁻⁶ (b) Main group metal complexes with formal Ch^{-II} centres. $^{8-11}$ (c) The reduction of O_2 , N_2O or S_8 with redox-active metal crown complex VI. 24

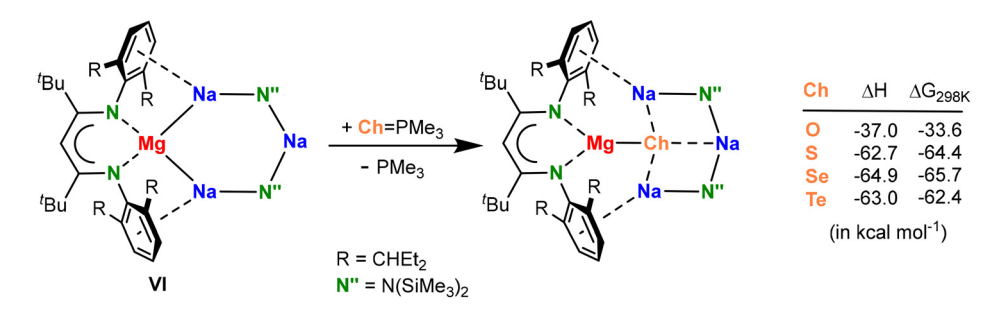
going down group 16 (P=O: 130 kcal mol⁻¹, P=S: 81 kcal mol⁻¹, P=Se: 64 kcal mol⁻¹, P=Te: 44 kcal mol⁻¹).³³ Consequently, reduction of R₃P=Ch to the respective R₃P and Ch²⁻ fragments becomes easier along the row Ch = O < S < Se < Te.

Use of Ph₃P=Ch reagents has been shown to be problematic in chalcogenide anion generation. The side-product PPh₃ cannot be separated easily from the reaction mixture, culminating in a drastic decrease of isolated product yields.8 Taking this into account, we chose to use Me₃P=Ch and Et₃P=Ch which have the advantage to produce volatile PMe3 and PEt3 which can be easily removed under vacuum. In all cases (Ch = O, S, Se, Te), DFT calculations support the thermodynamic feasibility for the formation of (BDI*)MgNa₃N"₂(Ch) from VI and Me₃P=Ch (Scheme 2). The reaction with Me₃P=O is the least exothermic while the reductions of the heavier phosphine chalcogenides release nearly double this energy.

In a general procedure, a solution of the redox-active metal crown complex (BDI*)MgNa₃N"₂ (VI) in cyclohexane-d₁₂ was reacted with one equivalent of Me₃P=Ch (or Et₃P=Ch) at room temperature. Upon stirring, the dark red colour of the reaction mixtures usually turned to yellow, indicative of Mg⁰ to Mg^{+II} conversion. The volatiles, including the phosphine sideproduct, were removed under high vacuum and the selectivity of the reaction was checked by 1H NMR.

Formation and trapping of the oxide dianion (VII-O)

Whereas the reduction of N₂O with VI is facile and cleanly produced (BDI*)MgNa3N"2(O) (VII-O), the reaction of VI with one equivalent of Me₃P=O only led to 33% conversion. The other 66% of VI remained untouched. Addition of two more equivalents of Me₃P=O finally led to full conversion of VI into one major, yet unknown product, which according to ¹H NMR chemical shifts is not the expected (BDI*)MgNa₃N"₂(O) (VII-O). The observed proton spectrum is identical to that of the product formed in reaction of [(BDI*)Mg]2Na2 with two equivalents of Me₃P=O (SI Fig. S50). This indicates that upon addition of Me₃P=O the inverse crown template VI dis-



Scheme 2 Calculated reaction enthalpies and free energies (kcal mol⁻¹; B3PW91-GD3BJ/def2tzvp//B3PW91-GD3BJ/def2svp) for reaction of VI with Me₃P=Ch to metal crown complexes of the Ch²⁻ anions.

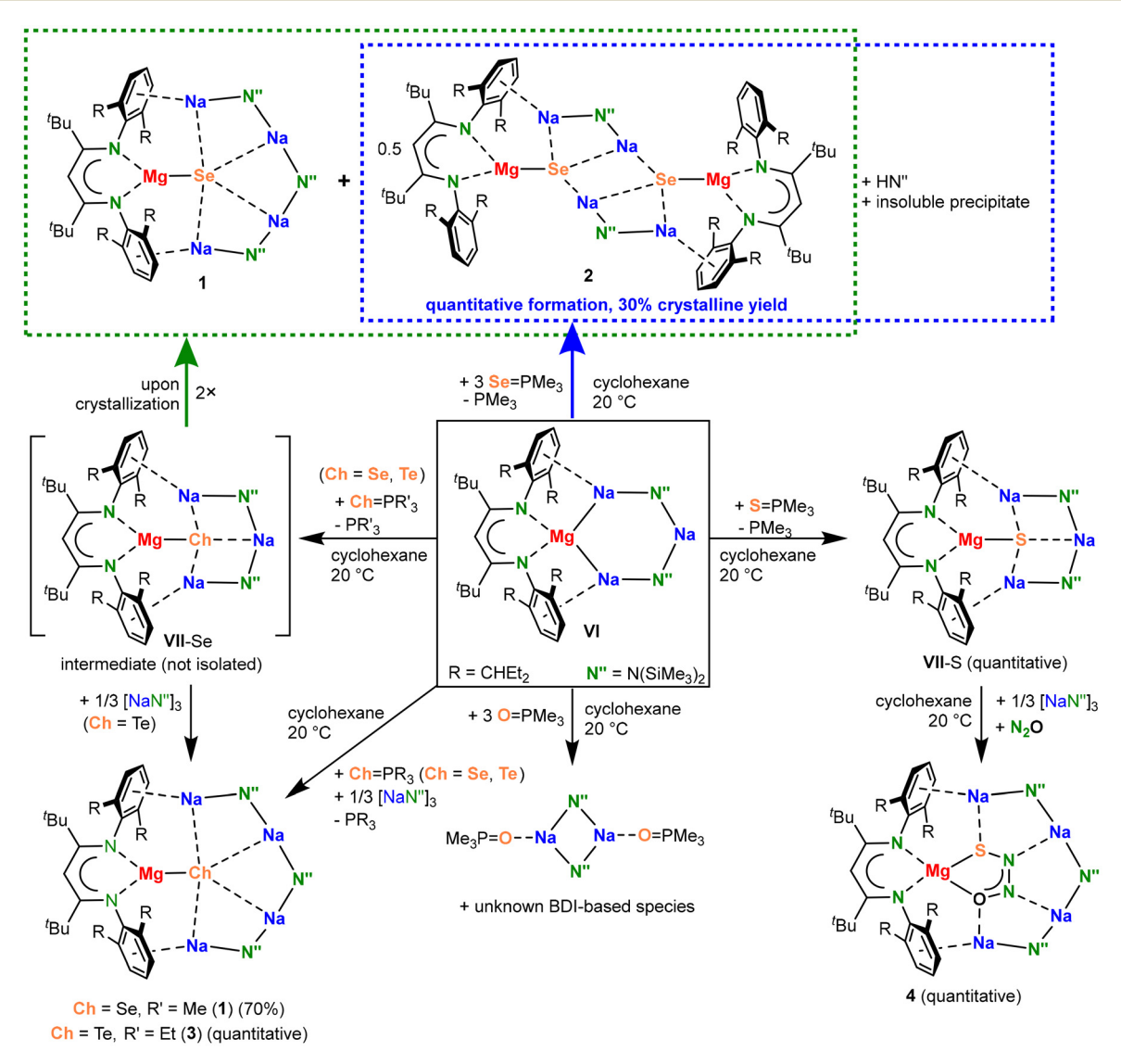
assembled and decomposed in $[(BDI^*)Mg]_2Na_2$ and NaN'' (Scheme 3). This is supported by NMR spectroscopy and X-ray diffraction analysis which are consistent with formation of $[(NaN'')(Me_3P=O)]_2$ (SI, Fig. S55). We earlier reported that **VI** disintegrates when dissolved in polar solvents as for example THF. Like THF, $Me_3P=O$ can act like a polar solvent, resulting in disassembly of **VI** and isolation of $[(NaN'')(Me_3P=O)]_2$.

Formation and trapping of the sulfide dianion (VII-S)

Exchange of Me₃P=O for the much less polar phoshine sulfide reagent, Me₃P=S, led to clean oxidation of **VI** and exclusive formation of (BDI*)MgNa₃N"₂(S) (**VII**-S) and PMe₃ (Scheme 3). Removing the solvent and phosphine under high vacuum gave a quantitative yield of essentially pure **VII**-S without the need of any further purification steps. Quantitative formation of the sulfide complex stands in contrast with the

modest yields reported for the reduction of Mg^I complexes with Ph₃P=S.⁸ Clean reactivity to VII-S can be explained by the stabilizing influence of the metal crown. In addition, Me₃P=S is much less polar than Me₃P=O and not able to destroy the metal crown by coordination.

The oxidation of Mg⁰ in VI with Me₃P—S is the privileged route for the generation of the sulfide complex VII-S. In the previously reported procedure,²⁴ it was found critical to react VI with exactly 0.125 equivalents of S₈ at low temperatures and at high dilution in order to prevent the formation of the persulfide complex (BDI*)MgNa₃N"₂(S₂) (VII-S₂). Especially on a smaller scale, it was found difficult to exactly add stoichiometric quantities of sulfur. The current synthetic route can be conveniently carried out in cyclohexane at room temperature using an excess of Me₃P—S. Any unreacted Me₃P—S remains as an insoluble solid which can be simply removed from the soluble product VII-S by filtration.



Scheme 3 Reactivity of VI with phosphine chalcogenides Ch—PMe₃ (Ch = O, S, Se) and Te—PEt₃.

Dalton Transactions Paper

Formation and trapping of the selenide and telluride dianions (1, 2, 3)

As R_3P =Se and R_3P =Te are both even less polar than R_3P =S and the P=Se and P=Te bonds are weaker than the P=S bond, controlled reduction of these reagents with VI should be straightforward.

The reduction of Me₃P=Se with VI led to the formation of various species among which complexes 1 and 2 are the main Mg selenide products (Scheme 3; raw product: Fig. S24 and S25). We presume that in a first step the expected product VII-Se is formed. However, in contrast to O²⁻ and S²⁻, the Se²⁻ dianion is too large to comfortably fit in the (BDI*)MgNa₃N"₂ crown. Concentrating and cooling the mother liquor led to crystallization of a ring enlargement product in which an additional NaN" is build in the ring: (BDI*)MgNa₄N"₃(Se) (1). Consequently, also a ring shrinkage product was found (BDI*) MgNa₂N"(Se) which crystallised as a dimer (2). As 1 and 2 are both well soluble in alkanes, purification by crystallization and washing procedures only resulted in very low yields. However, as shown in the synthesis of (BDI*)MgNa₄N"₃(ONNO) (VIII), ring expansion can be easily achieved by addition of 0.33 equivalents of trimeric (NaN")3 to the reaction mixture.24 Using the same approach, complex 1 could be isolated as a pure compound in 70% crystalline yield. We also observed that using a three-fold excess of Me₃P=Se, VI reacts selectively to 2, the complex depleted of NaN", which could be crystallized in 30% yield. This may be explained by the observation that (NaN")3 itself also reacts with Me3P=Se to give a highly insoluble white solid (likely Na₂Se₂) and HN" in which the origin of the proton remains unexplained. Using excess Me₃P=Se thus removes NaN" from VI, resulting in more selective formation of 2 which is depleted by one NaN" unit. Thus, also complex 2 could be obtained pure and was after crystallization isolated in 30% yield. Complexes 1 and 2 both exhibit ⁷⁷Se NMR signals with highly negative chemical shifts (1: -821.8 ppm, 2: -828.3 ppm; referenced to SeMe₂ as 0 ppm). These signals are considerably highfield-shifted when compared to Stasch's magnesium selenide complex III-Se (-764 ppm).8 Complex 1 should show two different ¹H NMR signals in a 2:1 ratio for the unequal N" ligands. The appearance of one signal indicates fast exchange between these

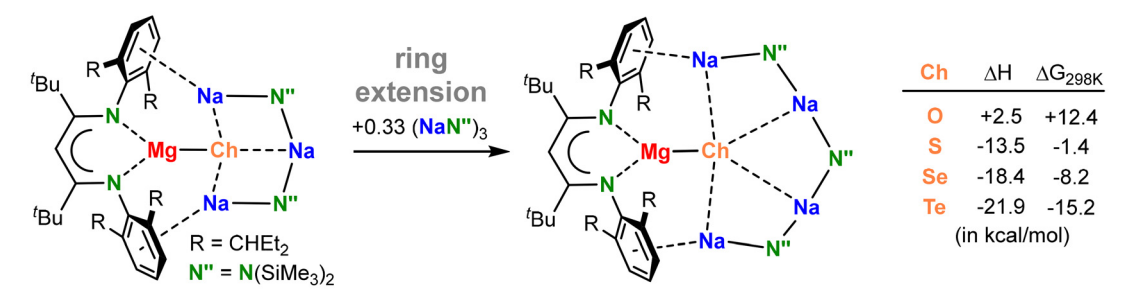
ligands. At -70 °C the signal broadens but decoalescence is not reached (Fig. S12).

In case of Te, we used Et₃P=Te as a reagent. The phosphine telluride Me₃P=Te is relatively unstable and easily decomposes to Me₃P and elemental Te. In contrast, the bulkier Et₃P=Te shows enhanced stability and PEt₃, which upon reduction is formed as a side-product, is still volatile enough for convenient removal under high vacuum. Reduction of Et₃P=Te with VI led to the isolation of the ring extension product (BDI*) MgNa₄N"₃(Te) (3, Scheme 3). In this case, the ring shrinkage product could not be isolated or identified, probably due to poor stability. As discussed above, addition of 0.33 equivalent of trimeric (NaN")3 at the start of the experiment, led to clean formation of the extended ring product and 3 could now be isolated in essentially quantitative yield. Similarly to the NMR shifts observed for the central Se²⁻ cores in 1 and 2, the ¹²⁵Te NMR spectrum of 3 features a noticeable high-field shifted resonance at -1902.3 ppm (referenced to TeMe2 as 0 ppm). Depending on the substituents, TeR2 compounds generally show ¹²⁵Te resonances between 0 and 500 ppm. The very negative chemical shift measured for 3 is also circa 500 to 1000 ppm more upfield than aluminium based tellurides with both single and double bonded Al-Te moieties. 12,34 Complex 3 should show two different ¹H NMR signals in a 2:1 ratio for the unequal N" ligands. The appearance of one signal indicates fast exchange between these ligands. At -70 °C the signal broadens but decoalescence is not reached (Fig. S37).

These investigations show that for the smaller chalcogenides, O²⁻ and S²⁻, the optimal ring size is defined by a tetrametallic MgNa₃-crown. The larger chalcogenides, Se²⁻ and Te²⁻, require the extended pentametallic MgNa₄-crown. DFT calculations, concerning such ring extension show that O2- encapsulation indeed prefers the smaller ring (Scheme 4 and Fig. S56) whereas the free energy difference for S²⁻ encapsulation in a small or large ring is close to zero. Ring extension for the larger anions, Se²⁻ and Te²⁻, becomes more exergonic with increasing anion size.

Reactivity of metal crown chalcogenide complexes with N₂O

Inspired by the ring extension from a MgNa₃-ring in (BDI*) MgNa₃N"₂(O) (VII-O) to the MgNa₄-ring in the hyponitrite complex (BDI*)MgNa₄N"₃(ONNO) (VIII) (Scheme 1),²⁴ com-



Scheme 4 Calculated reaction enthalpies and free energies (kcal mol⁻¹; B3PW91-GD3BJ/def2tzvp//B3PW91-GD3BJ/def2svp) for ring extension by addition of 0.33 equivalent of (NaN")3.

plexes VII-S, 1 and 3 were exposed to an N₂O atmosphere. In all three cases, the ¹H NMR spectra showed complete conversion of the reactants, but only for VII-S quantitative formation of the thiohyponitrite complex (BDI*)MgNa₄N"₃(SNNO) (4) was observed. Reaction of 1 and 3 with N₂O led to mixtures containing a myriad of products which could not be further isolated or identified. Complex 4 is a rare thiohyponitrite complex and the first isolated complex with a *cis*-SNNO²⁻ dianion trapped exclusively by main group metal cations. ^{35,36} Complex 4 should show three different ¹H NMR signals in a 1:1:1 ratio for the unequal N" ligands. The appearance of one signal indicates fast exchange between these ligands. At –70 °C decoalescence is reached (Fig. S45).

Crystal structures

Complex 1 crystallized C_2 -symmetric with the two-fold symmetry axis through the ligand backbone-CH, Mg, Se and one of the amide N atoms (Fig. 1a). The analogous Te complex 3 is

approximately C_2 -symmetric but does not possess crystallographic symmetry (Fig. 1b). The common feature of both compounds is the eight-membered Mg-Na-N-Na-N-Na-N-Na ring encapsulating the Ch²⁻ dianion. In contrast to **VI** in which the ring is held together by Mg-Na and Na-N bonds, the rings in **1** and **3** are formed by Ar···Na and Na-N bonding. While the Mg-Na bonds in **VI** are in the range of 3.261(2)-3.407(2) Å, the non-bonding Mg···Na1 distances in **1** measure 3.6568(6) Å. Those in **3** are slightly longer: 3.896(1)-3.951(1) Å. The latter lie within the range of the expanded metal crown complex **VIII** (Mg···Na 3.927(1)-3.965(1) Å). The Ar(centroid)····Na contacts in **1** and **3** vary from 2.625(1) to 2.705(1) Å and are of comparable length as similar interactions in **VI** (2.626(2)-2.735(2) Å) or **VIII** (2.600(1)-2.639(1) Å).

The Mg-Ch bonds of 2.4141(6) Å in 1 and 2.6068(6) Å in 3 are much shorter than the comparable Na-Ch distances varying from 2.8792(5) to 3.0084(6) Å in 1 or 3.0629(8) to 3.2259(8) Å in 3. The Mg-Ch bonds in 1 and 3 are also shorter

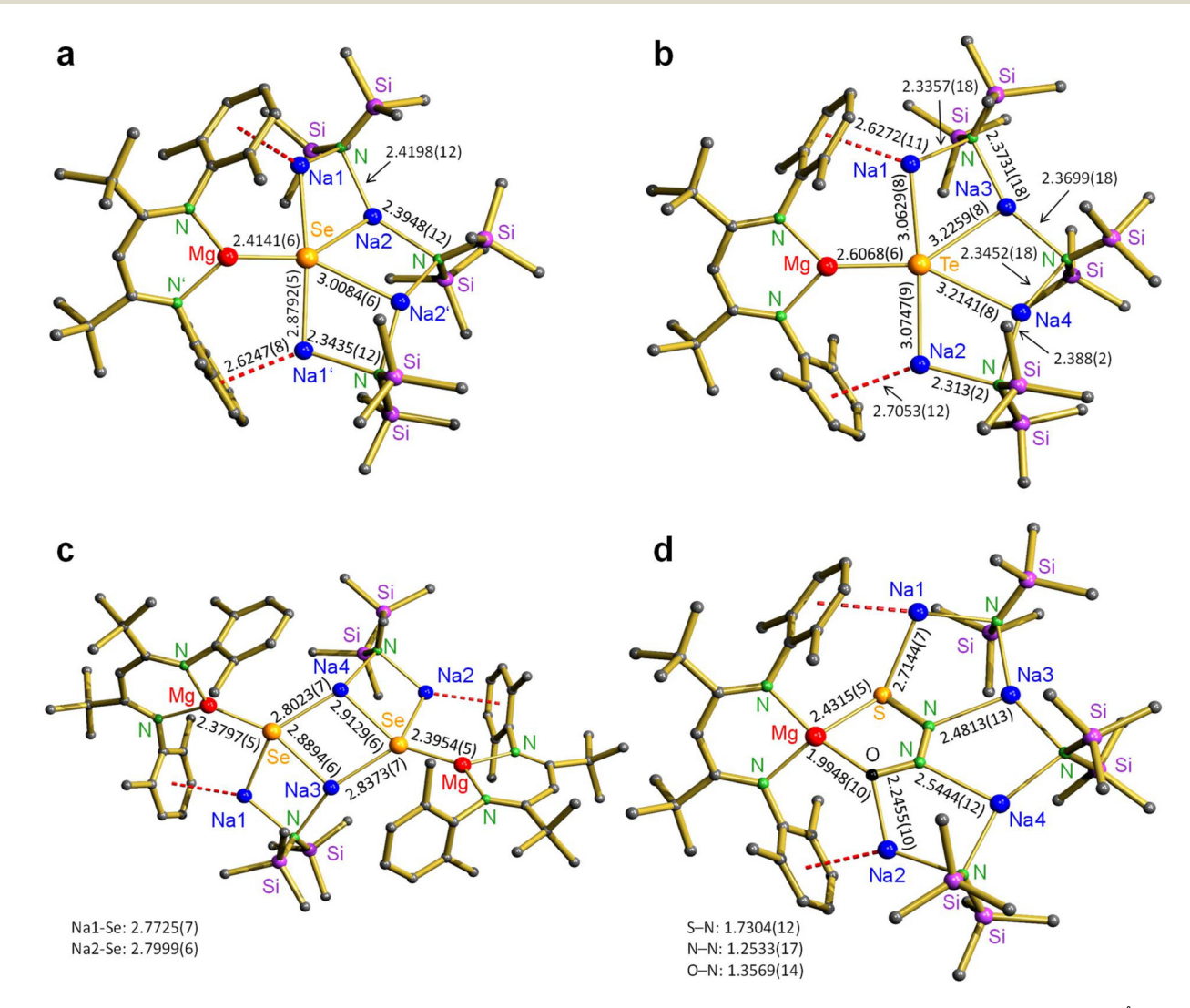


Fig. 1 Crystal structures; Et groups of the Et_2CH -substituents and H atoms are not shown for clarity. Bond distances shown in Å. (a) (BDI*) MgNa₄N"₃(Se) (1). (b) (BDI*)MgNa₄N"₃(Te) (3). (c) [(BDI*)MgNa₂N"(Se)]₂ (2). (d) (BDI*)MgNa₄N"₃(SNNO) (4).

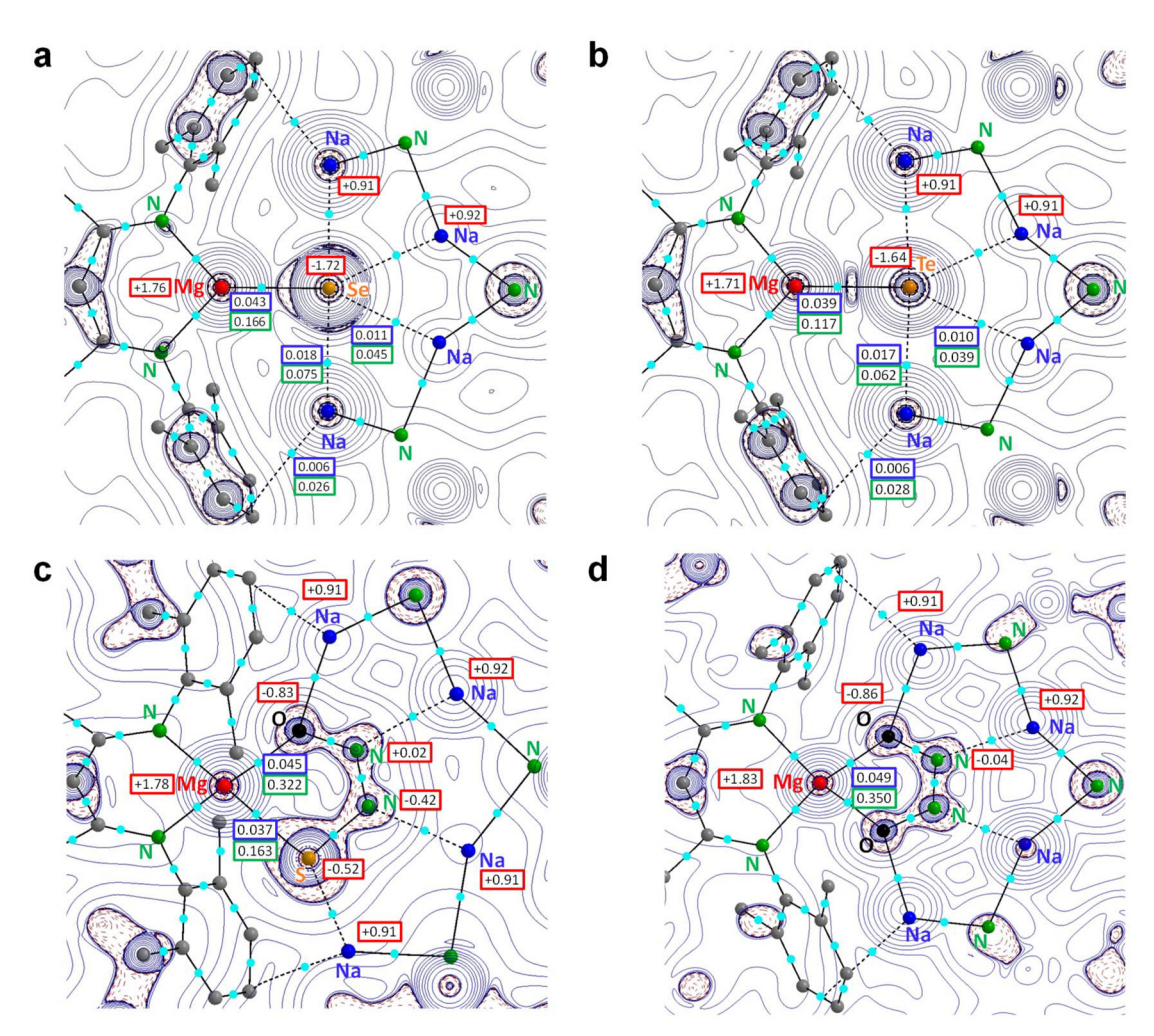


Fig. 2 NPA and Atoms-In-Molecules analyses. The Laplacian distributions show bcp's (light-blue) with ρ (r) (e B⁻³ in blue boxes), the Laplacian $\nabla^2 \rho$ (r) (e B⁻⁵ in green boxes) and NPA charges (red boxes). (a) (BDI*)MgNa₄N"₃(Se) (1). (b) (BDI*)MgNa₄N"₃(Te) (3). (c) (BDI*)MgNa₄N"₃(SNNO) (4). (d) (BDI*)MgNa₄N"₃(ONNO) (VIII).

than the sum of the covalence radii for Mg and Ch (Mg + Se: 2.61 Å, Mg + Te: 2.79 Å). The distances of similar length are observed in Parkin's magnesium selenide complex IV (2.404(3) and 2.408(3) Å) and Stasch's III-Se (2.3497(18)–2.4739(18) Å). The hitherto only compound with a Mg-Te bond that is crystallographically characterized, Mg[TeSi (SiMe₃)₃]₂(THF)₂, features considerably longer contacts (2.714 (1)–2.720(2) Å) than in 3. SiTe This is likely due to the monoanionic nature of (Me₃Si)₃SiTe compared to dianionic Te²⁻.

Complex 2 can be considered a dimer of (BDI*)MgNa₂N" (Se) units in which Se²⁻ is bound to Mg and chelated by a Na-N"-Na arm. The dimer has no crystallographic symmetry but is close to being C_2 -symmetric. The average Mg-Se (2.3876 Å) and Na-Se (2.8357 Å) distance in 2 are slightly shorter than those in 1 (average values: Mg-Se 2.4141 Å, Na-Se 2.9438 Å). This is due to the fact that Se²⁻ is five-coordinate in 1 but only four-coordinate in 2.

The thiohyponitrite complex **4** (Fig. 1d) crystallizes similarly to the hyponitrite complex **VIII**. ²⁴ It encapsulates a *cis*-SNNO²⁻

anion within an eight-membered Mg–Na1–N–Na3–N–Na4–N–Na2 ring and is bound by Mg–S, Mg–O, S–Na, O–Na and N–Na interactions The O–N–N–S bond distances in 4 are (Å): 1.357 (1)–1.253(2)–1.730(1). The O–N and N–N distances in 4 are very much comparable to those in the hyponitrite anion in complex **VIII** (O–N: 1.363(2), N–N: 1.261(2) Å), implying that replacement of O for S hardly influences O–N and N–N distances. In contrary, comparing the O–N–N–S bond distances in 4, 1.357(1)–1.253(2)–1.730(1), with those in a β -diketiminate Zn thiohyponitrite complex, 1.229(6)–1.306(7)–1.793(5), 35 shows significant differences that are likely related to differences between ionic bonding in 4 *versus* the more covalently bonding character in the Zn complex.

Computational studies

DFT calculations were conducted at the B3PW91-D3BJ/def2tzvp//B3PW91-D3BJ/def2svp level of theory which includes corrections for dispersion. The geometries for $\bf 1$ and $\bf 3$ have been optimized in C_2 -symmetry. They are in agreement with

Paper Dalton Transactions

those obtained by X-ray diffraction and only minor discrepancies are noted. The calculated Ch-Na bond lengths (1: Na1 2.780 Å, Na2 2.986 Å; 3: Na1/2 2.939 Å, Na3/4 3.132 Å) are slightly shorter than the experimentally found values (1: Na1 2.879 Å, Na2 3.008 Å; 3: Na1/2 3.063-3.075 Å, Na3/4 3.214-3.226 Å).

Atoms-In-Molecules (AIM) analysis confirms bonding between Mg-Ch and Ch-Na through the identification of bond paths and bond-critical points (bcp's) along the Mg-Ch and Ch-Na axes (Fig. 2a and b). The electron density $\rho(\mathbf{r})$ in the Mg-Ch bcp's is 2-4 times larger than in the Ch-Na bcp's underpinning the observations of X-ray diffraction, that Mg-Ch is the prominent bond. However, the associated electron density $\rho(\mathbf{r})$ and Laplacian $\nabla^2 \rho(\mathbf{r})$ in the bcp's are in all cases low, indicating a mainly ionic interaction. The Laplacian of the electron distribution shows a concentration of electron density at the Ch2- centres which is mainly polarized towards Mg2+ and only weakly directed to the nearest Na⁺ ions. The high electron density at the Ch²⁻ centres is further supported by Natural Population Analysis (NPA), which calculates a very low charge of -1.71 at Se and -1.64 at Te, and high positive charges at Mg (average +1.74) and Na (average +0.91), in line with ionic bonding between Ch²⁻, Mg²⁺ and Na⁺.

Fig. 2c shows the Laplacian and charge distribution for the thiohyponitrite complex 4. The SNNO²⁻ dianion is ionically bound in the metal crown with a total NPA charge of -1.75. The electron density on the Mg-S bond path is significantly smaller than that on the Mg-O bond path indicating that the Mg-O contact is the main bonding interaction.

Looking at the charge distribution within the thiohyponitrite anion (Fig. 2c) compared to that in the hyponitrite anion in VIII (Fig. 2d), it becomes clear that the latter has a major resonance form represented by O-N=N-O whereas in thiohyponitrite there is charge delocalization: ¬S−N=N−O¬ ↔ ¬S− N-N=O. Both N atoms in ONNO2- are nearly neutral whereas the N atom next to S in SNNO²⁻ carries a considerable negative charge.

Conclusion

The redox-active inverse crown complex VI is not stable in the presence of Me₃P=O. This is likely due to the high polarity of this phosphine oxide reagent which leads to loss of (NaN")2 from VI, resulting in [(NaN")(Me₃P=O)]₂, which could be identified, and [(BDI*)Mg]2Na2 which unselectively reduced Me₃P=O to a yet unidentified product. The much less polar heavier phosphine chalcogenides, R₃P=Ch (Ch = S, Se, Te), serve as excellent chalcogen transferring agents. Reduction of R₃P=Ch with the redox-active inverse crown VI led to inverse crown complexes with encapsulated Ch2- dianions (VII-S, 1 and 3). Choosing phosphine chalcogenides R₃P=Ch with R = Me or Et greatly simplified separation. Compared to solid PPh₃, the volatile phosphines PMe₃ and PEt₃ enabled high to quantitative product yields. Complex VII-S was previously prepared by reduction of S₈ with VI. However, a slight excess of

elemental sulfur led to contamination of the sulfide product VII-S with the disulfide VII-S₂. Since excess of R₃P=S does not disturb the clean formation of VII-S, this is the preferred method of preparation. The heavier chalcogenides Se2- and Te²⁻ are too large to be sufficiently stabilized by the tetrametallic MgNa₃-crown and required the formation of an extended pentametallic MgNa₄-crown. This was achieved by simple addition of 0.33 equivalents of (NaN")3 to the reaction mixtures. Reaction of (BDI*)MgNa₃N"₂(S) (VII-S) with N₂O in the presence of 0.33 equivalents (NaN")3 quantitatively yielded an inverse crown complex with the rare thiohyponitrite dianion cis-SNNO²⁻. The high electron density is delocalized over the four heteroatoms and, apart from the "S-N=N-O" resonance structure, features a significant S-N-N=O contribution. Current work focuses on expanding the scope of the reduceand-capture properties of VI to other groups of the periodic table and various small molecules.

Conflicts of interest

The authors declare no competing financial interest.

Data availability

Supplementary information: synthetic procedures, selected NMR spectra, details for crystal structure determination, details for computational work. See DOI: https://doi.org/ 10.1039/d5dt01896j.

CCDC 2429354, 2429355, 2429356, 2387081 and 2449050 contain the supplementary crystallographic data for this paper.40a-e

Acknowledgements

We acknowledge A. Roth for CHN analyses, M. A. Schmidt for support with the computational part and Dr. C. Färber and J. Schmidt for assistance with NMR analyses. We thank the Deutsche Forschungsgemeinschaft for funding (DFG: HA 3218/12-1).

References

- 1 C. J. Pedersen, J. Am. Chem. Soc., 1967, 89, 7017-7036.
- 2 C. J. Pedersen, Science, 1988, 241, 536-540.
- 3 C. J. Pedersen, Angew. Chem., Int. Ed. Engl., 1988, 27, 1021-1027.
- 4 A. R. Kennedy, R. E. Mulvey and R. B. Rowlings, Angew. Chem., Int. Ed., 1998, 37, 3180-3183.
- 5 R. E. Mulvey, Chem. Commun., 2001, 1049-1056.
- 6 R. E. Mulvey, Organometallics, 2006, 25, 1060–1075.
- 7 B. Li, C. Wölper and S. Schulz, CCDC 2290051. DOI: 10.5517/ccdc.csd.cc2gvzmy.

Dalton Transactions Paper

- 8 S. Burnett, R. Ferns, D. B. Cordes, A. M. Z. Slawin, T. van Mourik and A. Stasch, *Inorg. Chem.*, 2023, **62**, 16443–16450.
- 9 P. Ghosh and G. Parkin, Chem. Commun., 1996, 1239.
- M. J. Evans, M. D. Anker, C. L. McMullin, N. A. Rajabi and M. P. Coles, *Chem. Commun.*, 2021, 57, 2673–2676.
- 11 M. D. Anker and M. P. Coles, *Angew. Chem., Int. Ed.*, 2019, 58, 13452–13455.
- 12 X. Zhang and L. L. Liu, *J. Am. Chem. Soc.*, 2023, **145**, 15729–15734.
- 13 W. A. Howard and G. Parkin, *J. Am. Chem. Soc.*, 1994, **116**, 606–615.
- 14 D. Rabinovich and G. Parkin, *Inorg. Chem.*, 1995, **34**, 6341–6361
- 15 J. L. Kisko, T. Hascall and G. Parkin, *J. Am. Chem. Soc.*, 1997, **119**, 7609–7610.
- 16 C. Schneider, S. Ivlev and C. G. Werncke, *Eur. J. Inorg. Chem.*, 2023, **26**, e202200706.
- 17 W. Ren, G. Zi, D.-C. Fang and M. D. Walter, *J. Am. Chem. Soc.*, 2011, **133**, 13183–13196.
- 18 W. A. Howard, T. M. Trnka, M. Waters and G. Parkin, J. Organomet. Chem., 1997, 528, 95–121.
- 19 W. A. Howard and G. Parkin, *J. Organomet. Chem.*, 1994, 472, c1-c4.
- 20 J. H. Shin and G. Parkin, *Organometallics*, 1994, **13**, 2147–2149.
- 21 J. H. Shin and G. Parkin, *Organometallics*, 1995, **14**, 1104–1106.
- 22 V. J. Murphy and G. Parkin, *J. Am. Chem. Soc.*, 1995, 117, 3522–3528.
- 23 G. Giuffredi, T. Asset, Y. Liu, P. Atanassov and F. Di Fonzo, *ACS Mater. Au*, 2021, **1**, 6–36.
- 24 J. Maurer, L. Klerner, J. Mai, H. Stecher, S. Thum, M. Morasch, J. Langer and S. Harder, *Nat. Chem.*, 2025, 17, 703–709.
- 25 R. D. Shannon, Acta Crystallogr., Sect. A, 1976, 32, 751-767.
- 26 T. Chu, S. F. Vyboishchikov, B. Gabidullin and G. I. Nikonov, *Angew. Chem., Int. Ed.*, 2016, 55, 13306– 13311
- 27 B. J. Reeves and B. M. Boardman, *Polyhedron*, 2014, 73, 118–123.

- 28 S. M. Stuczynski, Y.-U. Kwon and M. L. Steigerwald, J. Organomet. Chem., 1993, 449, 167–172.
- 29 W. Imhof and G. Huttner, J. Organomet. Chem., 1993, 448, 247–253.
- 30 G. Hogarth, N. J. Taylor, A. J. Carty and A. Meyer, J. Chem. Soc., Chem. Commun., 1988, 834–836.
- 31 D. Belletti, D. Cauzzi, C. Graiff, A. Minarelli, R. Pattacini, G. Predieri and A. Tiripicchio, *J. Chem. Soc., Dalton Trans.*, 2002, 3160–3163.
- 32 T. Chu, S. F. Vyboishchikov, B. M. Gabidullin and G. I. Nikonov, *Inorg. Chem.*, 2017, **56**, 5993–5997.
- 33 N. Sandblom, T. Ziegler and T. Chivers, *Can. J. Chem.*, 1996, 74, 2363–2371.
- 34 H. Xu, A. Kostenko, C. Weetman, S. Fujimori and S. Inoue, Angew. Chem., Int. Ed., 2023, 62, e202216021.
- 35 N. J. Hartmann, G. Wu and T. W. Hayton, *Angew. Chem.*, *Int. Ed.*, 2015, **54**, 14956–14959.
- 36 M. Á. Baeza Cinco, G. Wu, N. Kaltsoyannis and T. W. Hayton, *Angew. Chem., Int. Ed.*, 2020, **59**, 8947–8951.
- 37 B. Cordero, V. Gómez, A. E. Platero-Prats, M. Revés, J. Echeverría, E. Cremades, F. Barragán and S. Alvarez, *Dalton Trans.*, 2008, 2832.
- 38 D. E. Gindelberger and J. Arnold, J. Am. Chem. Soc., 1992, 114, 6242–6243.
- 39 D. E. Gindelberger and J. Arnold, *Inorg. Chem.*, 1994, 33, 6293–6299.
- 40 (a) J. Maurer, L. Klerner, J. Langer, S. Harder, CCDC 2429354: Experimental Crystal Structure Determination, 2025, DOI: 10.5517/ccdc.csd.cc2mjy8d; (b) J. Maurer, L. Klerner, J. Langer, S. Harder, CCDC 2429355: Experimental Crystal Structure Determination, 2025, DOI: 10.5517/ccdc.csd.cc2mjy9f; (c) J. Maurer, L. Klerner, J. Langer, S. Harder, CCDC 2429356: Experimental Crystal Structure Determination, 2025, DOI: 10.5517/ccdc.csd. cc2mjybg; (d) J. Maurer, L. Klerner, J. Langer, S. Harder, CCDC 2387081: Experimental Crystal Determination, 2025, DOI: 10.5517/ccdc.csd.cc2l3ym9; (e) J. Maurer, L. Klerner, J. Langer, S. Harder, CCDC 2449050: Experimental Crystal Structure Determination, 2025, DOI: 10.5517/ccdc.csd.cc2n6fmy.